ISSN 1022 - 2502, E-ISSN 2408- 8528
Dhaka Univ. J. Sci. 72(2): 15-24, 2024 (July) DOI: https://doi.org/10.3329/dujs.v72i2.75465

Dynamic Complexity of a Discrete-time Prey-Predator Model with Mixed Functional Responses

Md. Jasim Uddin[1], Md. Shariful Islam[2], Mirza Fahim Ahmed[3] and Akram Hosen[3]

Department of Mathematics, University of Dhaka, Dhaka-1000, Bangladesh

(Received : 20 November 2023 ; Accepted : 25 June 2024)

Abstract

We examined the qualitative behaviors of a two-dimensional discrete-time predator-prey model with mixed functional responses. Mixed functional responses provide a more accurate representation of the complexities in predator-prey interactions compared to simple functional responses. Applying the center manifold theorem and bifurcation theory, we demonstrated analytically that the system passes through a Neimark-Sacker bifurcation and a Period-Doubling bifurcation in the interior of $\mathbb{R}^2$. The influence of step size parameters on the dynamics of the model is examined. Numerical simulations are used to display chaotic behavior, such as phase portraits, in addition to validating theoretical research. The parameter values have been discovered to have a significant impact on the dynamic behavior of the discrete prey-predator model. Eventually, the chaotic orbits are stabilized at an unstable fixed point via a hybrid control technique.

Keywords: Dynamical systems, Neimark-Sacker bifurcations, Period-Doubling bifurcations, Phase portrait, Chaos control

I. Introduction

Ecological systems are primarily defined by how organisms interact with the surrounding natural environment[1]. Because of their importance, population models are a major subject in many sciences. They examine how populations change over time. Malthus[2] is credited with being one of the first scientists to observe geometric population growth. His model, the exponential model, bears his name. Lotka[3] and Volterra[4] each completed independent studies that depict the prey-predator interaction. The Lotka–Volterra prey-predator model, which was the first significant development in this field, is the name given to this work. A basic reaction function proportional to the number of predators was employed by them. Later, to better simulate the phenomenon of predation, the model was expanded to incorporate three different types of functional responses for various species[5,6]. Subsequently, other adjustments to this model were proposed to create a more realistic prey-predator model by utilizing various types of functional response[7,8,9]. The study of bifurcation theory examines how dynamical models alter in relation to a control parameter. As a result, the system's behavior in relation to a control parameter is noted. Conversely, the bifurcation is the change in the qualitative structure of dynamical systems related to different values of the parameters. Numerous studies have been conducted on differential and difference equations[14,15]. A vast variety of population systems have been studied using differential and difference equations. Differential equations describing continuous-time systems suggest that discrete-time systems regulated by them make for more efficient computational systems for numerical simulations. Furthermore, where there are non-overlapping generations in the populations, discrete systems work better than continuous ones. In ecology, the population of many species evolves in discrete time steps because there is little overlap between generations. The discrete-time population models have also received attention recently since these can create more sophisticated and intriguing dynamical behaviors than continuous-time models and are better suited to simulate populations with non-overlapping generations. For instance, a 1-dimensional discrete-time autonomous system can display chaos, but a continuous-time arrangement requires chaos in at least a 3-dimensional autonomous system[22].

In mathematics, the predator-prey relationship is explained using a variety of models. A discrete predator-prey system of the Lotka–Volterra type with refuge effect, for example, has been studied for its bifurcation and dynamical behavior by Yildiz et al.[10]. The following discrete predator-prey model has been studied for its dynamic behavior and bifurcation by Li & Shao[11]:

$$\begin{cases} x_{t+1} = x_t e^{1-x_t-\frac{\alpha y_t}{x_t+y_t}}, \\ y_{t+1} = y_t e^{\beta\left(\frac{x_t}{x_t+y_t}-\gamma\right)}, \end{cases} \tag{1}$$

where the parameters α, β and γ are positive. The Neimark-Sacker bifurcation of the following discrete predator-prey model has been studied dynamically by Kangalgil[12]:

$$\begin{cases} x_{t+1} = \alpha x_t(1-x_t) - x_t y_t \left(\frac{x_t}{m+y_t}\right), \\ y_{t+1} = \frac{1}{\beta} x_t y_t, \end{cases} \tag{2}$$

where $\frac{x_t}{m+y_t}$ represents the Allee effect with m is the positive constants, α and β represent the growth rate of prey and predator respectively. The biological relevance of Allee effects, as reported in a manuscript, can vary

*Author for correspondence. e-mail: jasim.uddin@du.ac.bd

depending on the unique circumstances of the study and the species being investigated. Allee effects refer to a phenomenon in population ecology where the per capita growth rate of a population falls at low population densities, often leading to a critical threshold beyond which the population may struggle to exist or recover. Various types of functional responses are taken into account in formulating the mathematical model for both the predator and generalist predator in the study[23].

The Allee effect on the prey population affects the following discrete-time predator-prey system, which is described by Seval I.[13].

$$\begin{cases} x_{t+1} = rx_t(1-x_t) - \alpha x_t y_t \left(\frac{x_t}{m+y_t}\right), \\ y_{t+1} = bx_t y_t - dy_t, \end{cases} \tag{3}$$

where the Allee constant is applied to the prey population with parameter $m > 0$.

The biological significance of using mixed functional responses, such as the Holling Type I and Ivlev functional responses, in a discrete prey-predator model, is in portraying the intricacy of predator-prey interactions and their impact on population dynamics. Incorporating mixed functional responses in a discrete prey-predator model enhances its realism and biological relevance by accounting for the diversity of predator's foraging behavior and its ramifications for population dynamics, species coexistence, community structure, and ecosystem functioning. The objective of this study is to develop a discrete-time prey-predator model with an Ivlev and Holling type-I mixed functional response. We examine local asymptotic stability in detail of the fixed points in the suggested model. There are certain control parameters in the model. Any alteration to one of these control parameters will have an impact on the model's long-term behavior. We thus examine these impacts. Additionally, we provide a few numerical simulations to bolster and clarify our analytic findings. Our proposed model is given by the following system of differential equations

$$\begin{cases} \frac{dx}{dt} = r_1 x \ln\frac{k_1}{x} - \eta_1 xy\,, \\ \frac{dy}{dt} = \beta_1(1-e^{-a_1 x})y - \delta_1 y, \end{cases} \tag{4}$$

In this case, y represents the number of predators at any time, while x represents the number of prey in the population. In this system, in the absence of predators, the prey growth follows Gompertz law with an inherent growth rate of r_1 and a carrying capacity of k_1. The values of each parameter $r_1, k_1, \eta_1, \beta_1, a_1$ and δ_1 are positive. Furthermore, β_1 reflects the rates of predation, while r_1 signifies the intrinsic growth rate of the prey population. Additionally, the per capita predator mortality rate is represented by δ_1.

By utilizing the forward Euler technique, we can get the following discrete-time model with step size μ_1:

$$\begin{cases} x_{n+1} = x_n + \mu_1(r_1 x_n \ln\frac{k_1}{x_n} - \eta_1 x_n y_n), \\ y_{n+1} = y_n + \mu_1(\beta_1(1-e^{-a_1 x_n})y_n - \delta_1 y_n), \end{cases} \tag{5}$$

The structure of this paper is as follows. The stability criterion and existence condition for the fixed points of the system (5) are presented in Section II. In Section III, we demonstrate that system (5) admits an NS bifurcation and in Section IV system (5) admits a PD bifurcation in the interior of $\mathbb{R}^2$ under specific parametric conditions. We do our numerical simulations in Section V which contains the phase portraits and bifurcation diagrams. In Section VI, the hybrid control approach is used to control chaos about an unstable fixed point. Section VII contains a brief discussion at the end.

Remark: There are various reasons and benefits to adding a mixed functional response to traditional discrete-time prey-predator models. Compared to simple functional responses, mixed functional responses more accurately depict the intricacies of predator-prey interactions. Predator's eating behavior in the wild frequently varies according on prey population, prey species, and environmental circumstances. Models that include mixed functional responses can more accurately capture the dynamic character of predator-prey interactions. Models with diverse functional responses contribute to more accurate predictions regarding population dynamics and ecological stability by taking into consideration a wider variety of predator's feeding behaviors. Better management practices for natural ecosystems can be derived from prey-predator models that incorporate mixed functional responses. Overall, the goal of modeling and comprehending complex predator-prey interactions and ecosystem dynamics is to increase realism, flexibility, predictive accuracy, and ecological relevance. This drives the incorporation of mixed functional responses into traditional discrete-time prey-predator models.

II. Existence of Fixed Point and Stability Analysis

The nonnegative fixed points of the discrete prey-predator system (5) are computed in this section. The fixed points are $\varsigma_1(k_1, 0)$ and $\varsigma_2(x^* = -\frac{\ln\left[1-\frac{\delta_1}{\beta_1}\right]}{a_1}, y^* = \frac{r_1 \ln\left[\frac{k_1}{x^*}\right]}{\eta_1})$. The following table displays the existence condition of the fixed points of the system (5).

Table 1. Existence Condition for Fixed Points

Fixed Points	Conditions
ς_1	always
ς_2	$\delta_1 < \beta_1(1-e^{-a_1k_1})$

The Jacobian matrix of system (5) at any arbitrary point (x, y) is given by

$$J(x,y) = \begin{pmatrix} b_{11} & b_{12} \\ b_{21} & b_{22} \end{pmatrix}$$

where

$$b_{11} = 1 - r_1\mu_1 - y\eta_1\mu_1 + r_1\mu_1 \ln\left[\frac{k_1}{x}\right]$$
$$b_{12} = -x\eta_1\mu_1$$
$$b_{21} = a_1 e^{-a_1 x} y\beta_1\mu_1$$
$$b_{22} = 1 + \beta_1\mu_1 - e^{-a_1 x}\beta_1\mu_1 - \delta_1\mu_1$$

At $\varsigma_1(k_1, 0)$, the Jacobian matrix is given by

$$J\big(\varsigma_1(k_1,0)\big) = \begin{pmatrix} 1 - r_1\mu_1 & -k_1\eta_1\mu_1 \\ 0 & 1 + \beta_1\mu_1 - e^{-a_1k_1}\beta_1\mu_1 - \delta_1\mu_1 \end{pmatrix}$$

The eigenvalues of the above Jacobian matrix are $\lambda_1 = 1 - r_1\mu_1$ and $\lambda_2 = 1 + \beta_1\mu_1 - e^{-a_1k_1}\beta_1\mu_1 - \delta_1\mu_1$. Now we state the following lemma for the stability criterion of $\varsigma_1(k_1, 0)$.

Lemma 1. The following topological classification holds for the border fixed point $\varsigma_1(k_1, 0)$.

(i) The fixed point $\varsigma_1(k_1, 0)$ with $\delta_1 > \beta_1(1 - e^{-a_1k_1})$ is

(i.1) sink when $0 < \mu_1 < min\left\{\frac{2}{r_1}, \frac{2}{\delta_1 - \beta_1(1-e^{-a_1k_1})}\right\}$,

(i.2) source when $\mu_1 > max\left\{\frac{2}{r_1}, \frac{2}{\delta_1 - \beta_1(1-e^{-a_1k_1})}\right\}$,

(i.3) non-hyperbolic when $\mu_1 = \frac{2}{r_1}$ or $\mu_1 = \frac{2}{\delta_1 - \beta_1(1-e^{-a_1k_1})}$

(ii) The fixed point $\varsigma_1(k_1, 0)$ with $\delta_1 < \beta_1(1 - e^{-a_1k_1})$ is

(ii.1) source when $\mu_1 > \frac{2}{r_1}$,

(ii.2) saddle when $\mu_1 < \frac{2}{r_1}$,

(ii.3) non-hyperbolic when $\mu_1 = \frac{2}{r_1}$

(iii) The fixed point $\varsigma_1(k_1, 0)$ is no-hyperbolic when $\delta_1 = \beta_1(1 - e^{-a_1k_1})$.

One of the eigenvalues of $J\big(\varsigma_1(k_1,0)\big)$ is certainly -1 and the other may not be ± 1 when $\mu_1 = \frac{2}{r_1}$ or $\mu_1 = \frac{2}{\delta_1 - \beta_1(1-e^{-a_1k_1})}$. A PD bifurcation may happen, if the set of parameters changes around $\widetilde{PRD}^1_{\varsigma_1}$ or $\widetilde{PRD}^2_{\varsigma_1}$.

$$\widetilde{PRD}^1_{\varsigma_1} = \left\{(r_1, k_1, \eta_1, \beta_1, a_1, \delta_1, \mu_1) \in (0,\infty): \mu_1 = \frac{2}{r_1}, \mu_1 \neq \frac{2}{\delta_1 - \beta_1(1 - e^{-a_1k_1})}\right\}$$

or

$$\widetilde{PRD}^2_{\varsigma_1} = \left\{(r_1, k_1, \eta_1, \beta_1, a_1, \delta_1, \mu_1) \in (0,\infty): \mu_1 = \frac{2}{\delta_1 - \beta_1(1 - e^{-a_1k_1})}, \mu_1 \neq \frac{2}{r_1}\right\}$$

At $\varsigma_2(x^* = -\frac{\ln\left[1-\frac{\delta_1}{\beta_1}\right]}{a_1}, y^* = \frac{r_1 \ln\left[\frac{k_1}{x^*}\right]}{\eta_1})$ the characteristic equation changes as

$$F_{11}(\lambda) = \lambda^2 - (2 + \Gamma_1\mu_1)\lambda + (1 + \Gamma_1\mu_1 + \Delta_1{\mu_1}^2) = 0 \quad (6)$$

where

$$\Gamma_1 = -r_1 + \beta_1 - e^{-a_1x^*}\beta_1 - \delta_1$$

$$\Delta_1 = r_1\left(\left(-1 + e^{-a_1x^*}\right)\beta_1 + \delta_1 + a_1 e^{-a_1x^*}\beta_1 x^* \ln\left[\frac{k_1}{x^*}\right]\right)$$

So we state the following lemma for the stability conditions of the fixed point $\varsigma_2\left(x^* = -\frac{\ln\left[1-\frac{\delta_1}{\beta_1}\right]}{a_1}, y^* = \frac{r_1 \ln\left[\frac{k_1}{x^*}\right]}{\eta_1}\right)$.

Lemma 2. The following topological classification holds for the border fixed point $\varsigma_2\left(x^* = -\frac{\ln\left[1-\frac{\delta_1}{\beta_1}\right]}{a_1}, y^* = \frac{r_1 \ln\left[\frac{k_1}{x^*}\right]}{\eta_1}\right)$.

(i) source when

(i.1) ${\Gamma_1}^2 - 4\Delta_1 \geq 0$ and $\mu_1 > \frac{-\Gamma_1 + \sqrt{{\Gamma_1}^2 - 4\Delta_1}}{\Delta_1}$,

(i.2) ${\Gamma_1}^2 - 4\Delta_1 < 0$ and $\mu_1 > \frac{-\Gamma_1}{\Delta_1}$,

(ii) sink when

(ii.1) ${\Gamma_1}^2 - 4\Delta_1 \geq 0$ and $\mu_1 < \frac{-\Gamma_1 + \sqrt{{\Gamma_1}^2 - 4\Delta_1}}{\Delta_1}$,

(ii.2) ${\Gamma_1}^2 - 4\Delta_1 < 0$ and $\mu_1 < \frac{-\Gamma_1}{\Delta_1}$,

(iii) non-hyperbolic when

(iii.1) ${\Gamma_1}^2 - 4\Delta_1 \geq 0$ and $\mu_1 = \frac{-\Gamma_1 + \sqrt{{\Gamma_1}^2 - 4\Delta_1}}{\Delta_1}, \mu_1 \neq -\frac{2}{\Gamma_1}, -\frac{4}{\Gamma_1}$

(iii.2) ${\Gamma_1}^2 - 4\Delta_1 < 0$ and $\mu_1 = -\frac{4}{\Gamma_1}$,

(iv) otherwise saddle

Consider

$$\widetilde{PRD}_{\varsigma_2}^{1,2} = \left\{ (r_1, k_1, \eta_1, \beta_1, a_1, \delta_1, \mu_1) \in (0,\infty) : \mu_1 = \frac{-\Gamma_1 \pm \sqrt{{\Gamma_1}^2 - 4\Delta_1}}{\Delta_1} = \mu_{1\pm} \right\}$$

with ${\Gamma_1}^2 - 4\Delta_1 \geq 0, \mu_1 \neq -\frac{2}{\Gamma_1}, -\frac{4}{\Gamma_1}$

A PD bifurcation at $\varsigma_2\left(x^* = -\frac{\ln\left[1-\frac{\delta_1}{\beta_1}\right]}{a_1}, y^* = \frac{r_1 \ln\left[\frac{k_1}{x^*}\right]}{\eta_1}\right)$ may happen, if the set of parameters $(r_1, k_1, \eta_1, \beta_1, a_1, \delta_1, \mu_1)$ changes around $\widetilde{PRD}_{\varsigma_2}^{1,2}$.

Also, consider

$$\widetilde{NES}_{\varsigma_2}^{1} = \left\{ (r_1, k_1, \eta_1, \beta_1, a_1, \delta_1, \mu_1) \in (0,\infty) : \mu_1 = \frac{-\Gamma_1}{\Delta_1} = \mu_{1NS}, {\Gamma_1}^2 - 4\Delta_1 < 0 \right\}$$

when $(r_1, k_1, \eta_1, \beta_1, a_1, \delta_1, \mu_1)$ changes around $\widetilde{NES}_{\varsigma_2}^{1}$, the system experienced with NS bifurcation.

III. Neimark Sacker Bifurcation Analysis

Recent research has drawn a lot of attention to bifurcation in discrete dynamical systems because of these systems' complicated behavior. In population dynamics, bifurcations can occasionally be very unfavorable because of the possibility of extinction due to chaos. In a dynamical system, several kinds of bifurcations break away from a fixed point when a given parameter crosses its critical value. Because of the emergence of NS bifurcation, many dynamical aspects of a system can be explored. Bifurcation typically happens when a dynamical system's qualitative characteristics alter, or when the stability of a fixed point shifts. In this section, we have discussed about NS bifurcation at $\varsigma_2\left(x^* = -\frac{\ln\left[1-\frac{\delta_1}{\beta_1}\right]}{a_1}, y^* = \frac{r_1 \ln\left[\frac{k_1}{x^*}\right]}{\eta_1}\right)$ for model (5).

The bifurcation parameter in the analysis of the NSB is μ_1. Moreover, $\mu_1{}^*$ ($|\mu_1{}^*| \lll 1$) represents the perturbation of μ_1, and we examine the following perturbation of the model:

$$\begin{aligned} x_{n+1} &= x_n + (\mu_1 + \mu_1{}^*)\left(r_1 x_n \ln\frac{k_1}{x_n} - \eta_1 x_n y_n\right) = f_1(x_n, y_n, \mu_1), \\ y_{n+1} &= y_n + (\mu_1 + \mu_1{}^*)(\beta_1(1 - e^{-a_1 x_n})y_n - \delta_1 y_n) = f_2(x_n, y_n, \mu_1). \end{aligned} \quad (7)$$

Consider $u_n = x_n - x^*$ and $v_n = y_n - y^*$, then ς_2 is shifted to the origin. Applying Taylor series expansion to the functions f_1 and f_2 about $(u_n, v_n) = (0,0)$, the model (7) becomes

$$\begin{aligned} u_{n+1} &= \sigma_1 u_n + \sigma_2 v_n + \sigma_{11}{u_n}^2 + \sigma_{12} u_n v_n + \sigma_{22}{v_n}^2 + \sigma_{111}{u_n}^3 + \sigma_{112}{u_n}^2 v_n + \sigma_{122} u_n {v_n}^2 + \sigma_{222}{v_n}^3 + O((|u_n| + |v_n|)^4) \\ v_{n+1} &= \kappa_1 u_n + \kappa_2 v_n + \kappa_{11}{u_n}^2 + \kappa_{12} u_n v_n + \kappa_{22}{v_n}^2 + \kappa_{111}{u_n}^3 + \kappa_{112}{u_n}^2 v_n + \kappa_{122} u_n {v_n}^2 + \kappa_{222}{v_n}^3 + O((|u_n| + |v_n|)^4) \end{aligned} \quad (8)$$

where

$$\begin{aligned} \sigma_1 &= 1 - r_1\mu_1 \\ \sigma_2 &= -x^*\eta_1\mu_1 \\ \sigma_{11} &= -\frac{r_1\mu_1}{x^*} \\ \sigma_{12} &= -\eta_1\mu_1 \\ \sigma_{22} &= 0 \\ \sigma_{111} &= \frac{r_1\mu_1}{{x^*}^2} \\ \sigma_{112} &= 0 \\ \sigma_{222} &= 0 \\ \kappa_1 &= \frac{a_1 e^{-a_1 x^*} r_1 \beta_1 \mu_1 \ln\left[\frac{k_1}{x^*}\right]}{\eta_1} \\ \kappa_2 &= 1 - \delta_1\mu_1 + \beta_1\mu_1(1 - e^{-a_1 x^*}) \\ \kappa_{11} &= -\frac{{a_1}^2 e^{-a_1 x^*} r_1 \beta_1 \mu_1 \ln\left[\frac{k_1}{x^*}\right]}{\eta_1} \\ \kappa_{12} &= a_1 e^{-a_1 x^*}\beta_1\mu_1 \\ \kappa_{22} &= 0 \\ \kappa_{111} &= \frac{{a_1}^3 e^{-a_1 x^*} r_1 \beta_1 \mu_1 \ln\left[\frac{k_1}{x^*}\right]}{\eta_1} \\ \kappa_{112} &= {a_1}^2 e^{-a_1 x^*}\beta_1\mu_1 \\ \kappa_{122} &= 0 \\ \kappa_{222} &= 0 \end{aligned} \quad (9)$$

The characteristic equation linked to model (7)'s linearization at (0,0) is as follows

$$\lambda^2 - \breve{\varrho}_1(\mu_1{}^*)\lambda + \breve{\varrho}_2(\mu_1{}^*) = 0$$

where

$$\breve{\varrho}_1(\mu_1{}^*) = 2 + \Gamma_1\mu_1$$

$$\breve{\varrho}_2(\mu_1{}^*) = 1 + \Gamma_1\mu_1 + \Delta_1{\mu_1}^2$$

The characteristic equations' roots are

$$\lambda_{1,2}(\mu_1{}^*) = \frac{-\breve{\varrho}_1(\mu_1{}^*) \pm \sqrt{4\breve{\varrho}_2(\mu_1{}^*) - \left(\breve{\varrho}_1(\mu_1{}^*)\right)^2}}{2}$$

With $\left|\lambda_{1,2}(\mu_1{}^*)\right| = 1$, and $\mu_1{}^* = 0$, we obtain $\lambda_{1,2}(\mu_1{}^*) = [\breve{\varrho}_2(\mu_1{}^*)]^{\frac{1}{2}}$ and

$$l = \left[\frac{d|\lambda_{1,2}(\mu_1{}^*)|}{d\mu_1{}^*}\right]_{\mu_1{}^*=0} \neq 0$$

Additionally, with $\mu_1{}^* = 0, \lambda_{1,2}^i \neq 1, i = 1,2,3,4$, which is same as $\breve{\varrho}_1(\mu_1{}^*) \neq -2, -1,1,2$.

For analyzing the normal structure, consider $\gamma = Im(\lambda_{1,2})$ and $\delta = Re(\lambda_{1,2})$. Also using $T = \begin{bmatrix} 0 & 1 \\ \gamma & \delta \end{bmatrix}$ and $\begin{bmatrix} u_n \\ v_n \end{bmatrix} = T\begin{bmatrix} \overline{x_n} \\ \overline{y_n} \end{bmatrix}$ model (8) becomes

$$\overline{x_{n+1}} = \delta\overline{x_n} - \gamma\overline{y_n} + f_2(\overline{x_n}, \overline{y_n})$$

$$\overline{y_{n+1}} = \gamma\overline{x_n} + \delta\overline{y_n} + g_2(\overline{x_n}, \overline{y_n}) \quad (10)$$

For Neimark-Sacker Bifurcation to occur, we need the discriminatory quantity $\mathcal{M}$ to be nonzero.

$$\mathcal{M} = -Re\left[\frac{(1-2\bar{\lambda})\bar{\lambda}^2}{1-\lambda}\vartheta_{11}\vartheta_{20}\right] - \frac{1}{2}|\vartheta_{11}|^2 - |\vartheta_{02}|^2 + Re(\bar{\lambda}\,\vartheta_{21}), \quad (11)$$

where

$$\vartheta_{20} = \frac{1}{8}\delta(2\kappa_{22} - \delta\sigma_{22} - \sigma_{12} + 4\gamma\sigma_{22}) + \frac{1}{4}\gamma\sigma_{12} + \frac{1}{8}\delta i(4\gamma\sigma_{22} - 2\sigma_{22} - 2\delta\sigma_{22}) + \frac{1}{8}i(4\gamma\kappa_{22} + 2\gamma^2\sigma_{22} - 2\sigma_{11}) + \frac{1}{8}\kappa_{12} + \frac{\delta\sigma_{11} - 2\kappa_{11} + \delta^3\sigma_{22} - \delta^2\kappa_{22} - \delta^2\sigma_{12} + \delta\kappa_{12}}{4\gamma},$$

$$\vartheta_{11} = \frac{1}{2}\gamma(\kappa_{22} - \delta\sigma_{22}) + \frac{1}{2}i(\gamma^2\sigma_{22} + \sigma_{11} + \delta\sigma_{12} + \delta^2\sigma_{22}) + \frac{\kappa_{11} - \delta\sigma_{11} + \delta\kappa_{12} - \delta^2\sigma_{12}}{2\gamma} - \frac{\delta^2\kappa_{22} - \delta^3\sigma_{22}}{\gamma},$$

$$\vartheta_{02} = \frac{1}{4}\gamma(2\delta\sigma_{22} + \sigma_{12} + \kappa_{22}) + \frac{1}{4}i(\kappa_{12} + 2\delta\kappa_{22} - 2\delta\sigma_{12} - \sigma_{11}) - \frac{\kappa_{11} - \delta\sigma_{11} + \delta\kappa_{12} - \delta^2\sigma_{12}}{4\gamma} + \frac{1}{4}\sigma_{22}i(\gamma^2 - 3\delta^2) + \frac{\delta^2\kappa_{22} - \delta^3\sigma_{22}}{4\gamma}$$

$$\vartheta_{21} = \frac{3}{8}\kappa_{222}(\gamma^2 + \delta^2) + \frac{1}{8}\kappa_{112} + \frac{1}{4}\delta\sigma_{112} + \frac{1}{4}\delta\kappa_{122} + \sigma_{122}\left(\frac{1}{8}\gamma^2 + \frac{3}{8}\delta^2 - \frac{1}{4}\delta\right) + \frac{3}{8}\sigma_{111} + \frac{3}{8}\sigma_{222}i(\gamma^2 + 2\delta^2) + \frac{3}{8}\sigma_{122}\gamma\delta i - \frac{1}{8}\kappa_{122}\gamma i - \frac{3}{8}\kappa_{222}\gamma\delta i - \frac{3\kappa_{111} - 3\delta\sigma_{111} + 3\delta\kappa_{112} - 3\delta^2\sigma_{112}}{8\gamma}i - \frac{3\delta^2\kappa_{122} - 3\delta^3\sigma_{122} + 3\delta^3\kappa_{222} - 3\delta^4\sigma_{222}}{8\gamma}i \quad (12)$$

The following outcome can be obtained from the analysis above.

Theorem 1. The model (5) is experienced with NS bifurcation if $\mathcal{M} \neq 0$ with μ_1 varies near the set $\widetilde{NES}_{\varsigma_2}^1$. Additionally, with $\mathcal{M} < 0$ ($\mathcal{M} > 0$) the invariant closed orbits to split off from $\varsigma_2\left(x^* = -\frac{\ln\left[1-\frac{\delta_1}{\beta_1}\right]}{a_1}, y^* = \frac{r_1\ln\left[\frac{k_1}{x^*}\right]}{\eta_1}\right)$ for $\mu_1{}^* > 0$ ($\mu_1{}^* < 0$).

IV. Period-Doubling Bifurcation Analysis

This section uses the center manifold theorem and bifurcation theory[20,21,24] to examine the PD bifurcation at $\varsigma_2\left(x^* = -\frac{\ln\left[1-\frac{\delta_1}{\beta_1}\right]}{a_1}, y^* = \frac{r_1\ln\left[\frac{k_1}{x^*}\right]}{\eta_1}\right)$ of the discrete model (5).

The bifurcation parameter in the analysis of the PD bifurcation is μ_1. Moreover, $\mu_1{}^*$ ($|\mu_1{}^*| \lll 1$) represents the perturbation of μ_1, and we examine the following perturbation of the model.

$$x_{n+1} = x_n + (\mu_1 + \mu_1{}^*)\left(r_1x_n\ln\frac{k_1}{x_n} - \eta_1x_ny_n\right) = f_1(x_n, y_n, \mu_1),$$

$$y_{n+1} = y_n + (\mu_1 + \mu_1{}^*)(\beta_1(1 - e^{-a_1x_n})y_n - \delta_1y_n) = f_2(x_n, y_n, \mu_1). \quad (13)$$

Consider $u_n = x_n - x^*$ and $v_n = y_n - y^*$, then ς_2 is shifted to the origin. Applying Taylor series expansion to the functions f_1 and f_2 about $(u_n, v_n, \mu_1{}^*) = (0,0,0)$, the model (13) becomes

$$u_{n+1} = \sigma_1u_n + \sigma_2v_n + \sigma_{11}{u_n}^2 + \sigma_{12}u_nv_n + \sigma_{13}u_n\mu_1{}^* + \sigma_{23}v_n\mu_1{}^* + \sigma_{111}{u_n}^3 + \sigma_{112}{u_n}^2v_{n+\sigma_{113}{u_n}^2\mu_1{}^*} + \sigma_{123}u_nv_n\mu_1{}^* + O((|u_n| + |v_n| + |\mu_1{}^*|)^4),$$

$$v_{n+1} = \kappa_1u_n + \kappa_2v_n + \kappa_{11}{u_n}^2 + \kappa_{12}u_nv_n + \kappa_{22}{v_n}^2 + \kappa_{13}u_n\mu_1{}^* + \kappa_{23}v_n\mu_1{}^* + \kappa_{111}{u_n}^3 + \kappa_{112}{u_n}^2v_n + \kappa_{113}{u_n}^2\mu_1{}^* + \kappa_{123}u_nv_n\mu_1{}^* + \kappa_{223}{v_n}^2\mu_1{}^* + O((|u_n| + |v_n| + |\mu_1{}^*|)^4) \quad (14)$$

where

$$\sigma_{13} = -r_1$$

$$\sigma_{23} = -x^*\eta_1$$

$$\sigma_{113} = -\frac{r_1}{x^*}$$

$$\sigma_{123} = -\eta_1$$

$$\kappa_{13} = \frac{a_1 e^{-a_1 x^*} r_1 \beta_1 \ln\left[\frac{k_1}{x^*}\right]}{\eta_1}$$

$$\kappa_{23} = \beta_1 - e^{-a_1 x^*}\beta_1 - \delta_1$$

$$\kappa_{113} = -\frac{{a_1}^2 e^{-a_1 x^*} r_1 \beta_1 \ln\left[\frac{k_1}{x^*}\right]}{\eta_1}$$

$$\kappa_{123} = a_1 e^{-a_1 x^*}\beta_1 \tag{15}$$

We assume $T = \begin{bmatrix} \sigma_2 & \sigma_2 \\ -1-\sigma_1 & \lambda_2 - \sigma_1 \end{bmatrix}$ and T is invertible obviously. Prosecute $\begin{bmatrix} u_n \\ v_n \end{bmatrix} = T\begin{bmatrix} \overline{x_n} \\ \overline{y_n} \end{bmatrix}$, the model (14) becomes

$$\overline{x_{n+1}} = -\overline{x_n} + f_2(\overline{x_n}, \overline{y_n}, {\mu_1}^*)$$

$$\overline{y_{n+1}} = \lambda_2 \overline{y_n} + g_2(\overline{x_n}, \overline{y_n}, {\mu_1}^*) \tag{16}$$

The center manifold of (16) at (0,0) around ${\mu_1}^* = 0$, can be written as follows

$$U^c(0,0,0) = \left\{(\overline{x_n}, \overline{y_n}, {\mu_1}^*) \in \mathbb{R}^3 : \overline{y_{n+1}} = \overline{\sigma_1}\,\overline{x_n}^2 + \overline{\sigma_2}\,\overline{x_n}{\mu_1}^* + O((|\overline{x_n}| + |{\mu_1}^*|)^3)\right\}$$

where

$$\overline{\sigma_1} = \frac{\sigma_2[(1+\sigma_1)\sigma_{11} + \sigma_2\kappa_{11}]}{1-\lambda_2^2} + \frac{\kappa_{22}(1+\sigma_1)^2}{1-\lambda_2^2} - \frac{(1+\sigma_1)[\sigma_{12}(1+\sigma_1) + \sigma_2\kappa_{12}]}{1-\lambda_2^2},$$

$$\overline{\sigma_2} = \frac{(1+\sigma_1)[\sigma_{23}(1+\sigma_1) + \sigma_2\kappa_{23}]}{\sigma_2(1+\lambda_2)^2} - \frac{(1+\sigma_1)[\sigma_{13} + \sigma_2\kappa_{13}]}{(1+\lambda_2)^2}, \tag{17}$$

The center manifold can be rewritten as follows

$$\overline{x_{n+1}} = -\overline{x_n} + h_1\overline{x_n}^2 + h_2\overline{x_n}{\mu_1}^* + h_3\overline{x_n}^2{\mu_1}^* + h_4\overline{x_n}{\mu_1}^{*2} + h_5\overline{x_n}^3 + O((|\overline{x_n}| + |{\mu_1}^*|)^3) = F(\overline{x_n}, {\mu_1}^*), \tag{18}$$

where

$$h_1 = \frac{\overline{\sigma_2}[(\lambda_2 - \overline{\sigma_1})\sigma_{11} - \overline{\sigma_2}\kappa_{11}]}{1+\lambda_2} - \frac{\kappa_{22}(1+\overline{\sigma_1})^2}{1+\lambda_2} - \frac{(1+\overline{\sigma_1})[(\lambda_2 - \overline{\sigma_1})\sigma_{12} - \overline{\sigma_2}\kappa_{12}]}{1+\lambda_2}$$

$$h_2 = \frac{(\lambda_2 - \overline{\sigma_1})\sigma_{13} - \overline{\sigma_2}\kappa_{13}}{1+\lambda_2} - \frac{(1+\overline{\sigma_1})[(\lambda_2 - \overline{\sigma_1})\sigma_{23} - \overline{\sigma_2}\kappa_{23}]}{1+\lambda_2}$$

$$h_3 = \frac{[(\lambda_2-\sigma_1)\sigma_{23} - \sigma_2\kappa_{23}](\lambda_2 - \sigma_1)\overline{\sigma_1}}{\sigma_2(1+\lambda_2)} + \frac{(\lambda_2-\sigma_1)\overline{\sigma_1}\sigma_{13} - \sigma_2\kappa_{13} + \sigma_2[(\lambda_2-\sigma_1)\sigma_{113} - \sigma_2\kappa_{113}] - \kappa_{223}(1+\sigma_1)^2}{1+\lambda_2} + \frac{2\sigma_2\overline{\sigma_2}[(\lambda_2-\sigma_1)\sigma_{11} - \sigma_2\kappa_{11}]}{1+\lambda_2} - \frac{(1+\sigma_1)[(\lambda_2-\sigma_1)\sigma_{123} - \sigma_2\kappa_{123}]}{1+\lambda_2} - \frac{2\kappa_{22}\overline{\sigma_2}(1+\sigma_1)(\lambda_2-\sigma_1)}{1+\lambda_2} + \frac{\overline{\sigma_2}[(\lambda_2-\sigma_1)\sigma_{12} - \sigma_2\kappa_{12}](\lambda_2 - 1 - 2\sigma_1)}{1+\lambda_2}$$

$$h_4 = \frac{\overline{\sigma_2}[(\lambda_2-\sigma_1)\sigma_{13} - \sigma_2\kappa_{13}]}{1+\lambda_2} + \frac{[(\lambda_2-\sigma_1)\sigma_{23} - \sigma_2\kappa_{23}](\lambda_2-\sigma_1)\overline{\sigma_2}}{1+\lambda_2} + \frac{2\sigma_2\overline{\sigma_2}[(\lambda_2-\sigma_1)\sigma_{11} - \sigma_2\kappa_{11}]}{1+\lambda_2} + \frac{2\kappa_{22}\overline{\sigma_2}(1+\sigma_1)(\lambda_2-\sigma_1)}{1+\lambda_2} + \frac{\overline{\sigma_2}[(\lambda_2-\sigma_1)\sigma_{12} - \sigma_2\kappa_{12}](\lambda_2 - 1 - 2\sigma_1)}{1+\lambda_2}$$

$$h_5 = \frac{2\sigma_2\overline{\sigma_1}[(\lambda_2-\sigma_1)\sigma_{11} - \sigma_2\kappa_{11}] + \overline{\sigma_2}^2[(\lambda_2-\sigma_1)\sigma_{111} - \sigma_2\kappa_{111}]}{1+\lambda_2} + \frac{2\kappa_{22}\overline{\sigma_1}(\lambda_2-\sigma_1)(1+\sigma_1)}{1+\lambda_2} + \frac{\overline{\sigma_1}[(\lambda_2-\sigma_1)\sigma_{11} - \sigma_2\kappa_{11}](\lambda_2 - 1 - 2\sigma_1)}{1+\lambda_2} - \frac{\overline{\sigma_2}(1+\sigma_1)[(\lambda_2-\sigma_1)\sigma_{112} - \sigma_2\kappa_{112}]}{1+\lambda_2} \tag{19}$$

We require the two discriminatory quantities for PD bifurcation.

$$\mathcal{H}_1 = \left(\frac{\partial^2 F}{\partial\overline{x_n}\partial{\mu_1}^*} + \frac{1}{2}\frac{\partial F}{\partial{\mu_1}^*}\frac{\partial^2 F}{\partial\overline{x_n}^2}\right)|_{(0,0)},$$

$$\mathcal{H}_2 = \left(\frac{1}{6}\frac{\partial^3 F}{\partial\overline{x_n}^3} + \left(\frac{1}{2}\frac{\partial^2 F}{\partial\overline{x_n}^2}\right)^2\right)|_{(0,0)}.$$

We can conclude the above analysis in the following theorem.

Theorem 2. The model (5) is experienced with PD bifurcation if $\mathcal{H}_1 \neq 0$ and $\mathcal{H}_2 \neq 0$ with μ_1 varies near the set $\widetilde{PRD}_{\varsigma_2}^{1,2}$. Additionally, with $\mathcal{H}_2 > 0$ ($\mathcal{H}_2 < 0$) the period-two orbits to split off from $\varsigma_2\left(x^* = -\frac{\ln\left[1-\frac{\delta_1}{\beta_1}\right]}{a_1}, y^* = \frac{r_1 \ln\left[\frac{k_1}{x^*}\right]}{\eta_1}\right)$ are stable (unstable).

V. Quantitative Study

Arbitrary data are utilized to describe the analytical results. Once more, it's noted that the parameters within the system do not directly reflect real-life scenarios. Therefore, the primary features are examined through simulations outlined here, which should be interpreted qualitatively rather than quantitatively. Numerical simulation work has been done in this section to offer phase pictures and bifurcation diagrams of the system (5) which both validate our theoretical findings and highlight some new, intriguing, complicated dynamical behaviors that the system (5) exhibits. We have used iterative techniques for the numerical simulations of our study. We consider the following illustrations.

Illustrations 1: By choosing $r_1 = 1.45, k_1 = 1.16, a_1 = 1.25, \eta_1 = 1.10, \beta_1 = 1.1, \delta_1 = 0.01$ and μ_1 varies in the range $1.1612 \leq \mu_1 \leq 1.2831$. We get a fixed point $(x_0, y_0) = (0.00730599, 6.67986)$ and PD bifurcation point is $\mu_{1PD} = 1.26969$. The associated eigenvalues are $\lambda = -1,\ 0.925114$. Figure 1 illustrates the model's trajectory as it transitions from a fixed point to a PD

bifurcation and then to a chaotic attractor. The phase portrait corresponding to Figure 1 for different values of μ_1 are displayed in Figure 2. This essentially illustrates the bifurcation of a smooth, unchanging closed curve into a chaotic attractor from a stable fixed point.

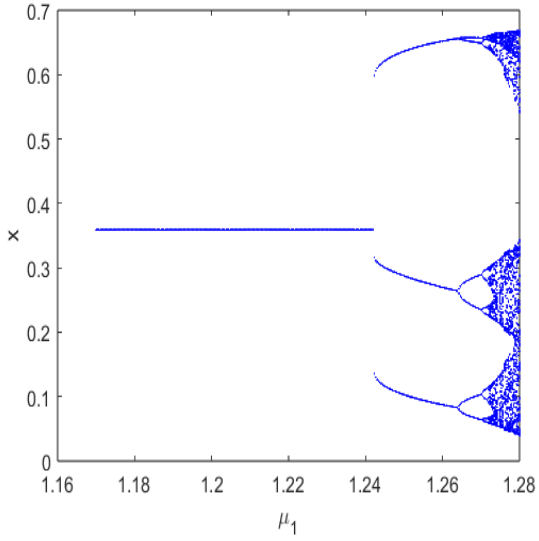

(a) **Diagram of Bifurcations for x_n.**

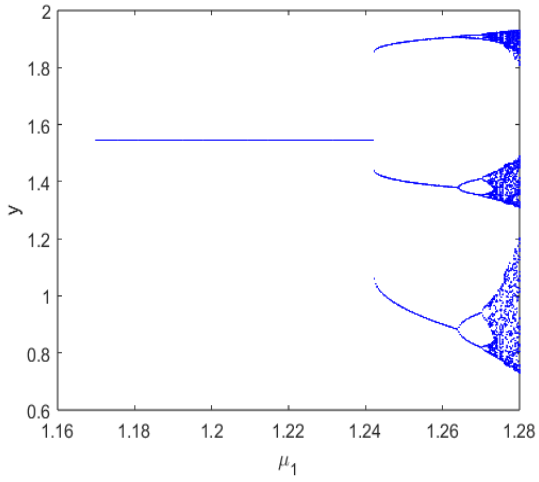

(b) **Diagram of Bifurcations for y_n.**

Fig. 1. Diagram of Bifurcations of model (5) with $r_1 = 1.45, k_1 = 1.16, a_1 = 1.25, \eta_1 = 1.10, \beta_1 = 1.1, \delta_1 = 0.01$ and μ_1 varies in the range $1.1612 \leq \mu_1 \leq 1.2831$.

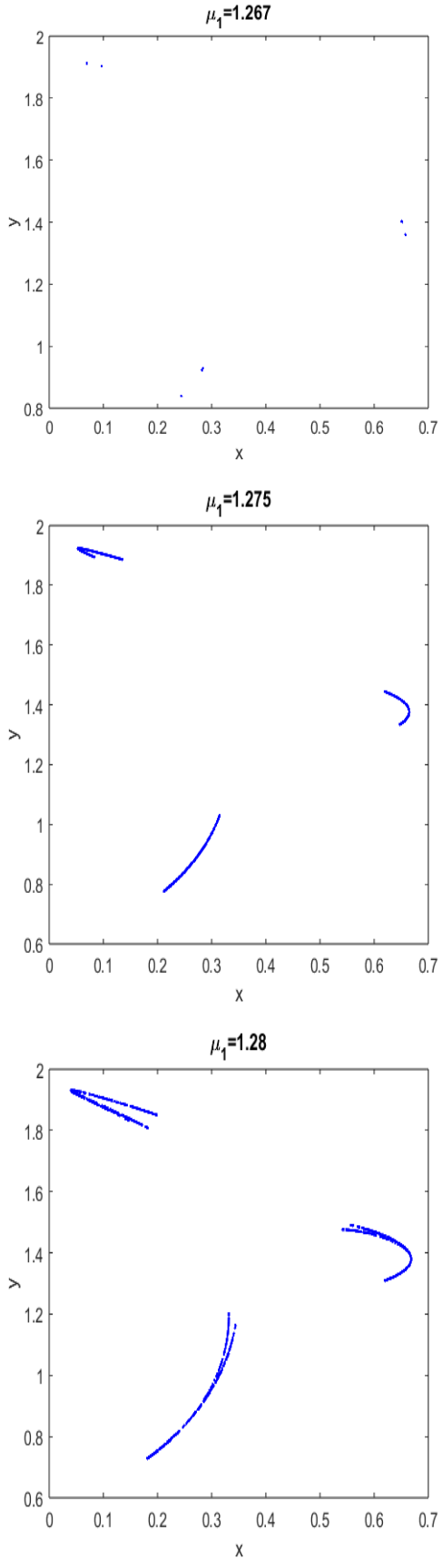

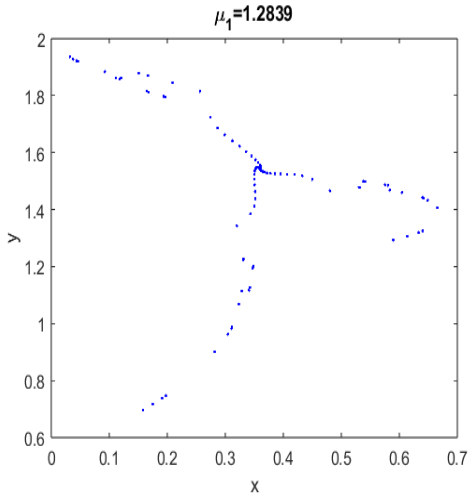

Fig 2. Phase portraits of the model (5) with $r_1 = 1.45, k_1 = 1.16, a_1 = 1.25, \eta_1 = 1.10, \beta_1 = 1.1, \delta_1 = 0.01$ for different choices of μ_1. (a) Phase diagram for $\mu_1 = 1.267$, (b) Phase diagram for $\mu_1 = 1.275$, (c) Phase diagram for $\mu_1 = 1.28$, (d) Phase diagram for $\mu_1 = 1.2839$.

VI. Chaos Control

It is the goal of dynamical systems to avoid chaos and optimize the system concerning a performance criterion. In a discrete prey-predator model, chaos control is essential to comprehending and controlling ecological systems. Nonlinear interactions between prey and predator populations in such models can lead to chaos. Even in situations where deterministic equations control the system, seemingly random and unpredictable behavior is referred to be chaos. Controlling chaos in discrete-time systems has drawn a lot of attention from researchers lately, and useful techniques can be applied in a variety of settings, including turbulence, physics labs, communications, and medical sectors[16]. Several techniques, including the pole-placement approach[17](Ott-Grebogi-Yorke (OGY) method), hybrid control method[18], and state feedback control method[19], can be used to achieve chaos control in discrete-time models. We just focus on the hybrid control approach, which is based on parameter perturbation and feedback control technique, in this part.

We use the hybrid control feedback mechanism[18] to control chaos in the system *(5)*. We write our uncontrolled system (5) using a hybrid control technique.

$$X_{n+1} = G(X_n, \mu_1) \tag{20}$$

Where μ_1 is the bifurcation parameter. Applying a hybrid control strategy to (20), we get,

$$X_{n+1} = \tau\, G(X_n, \mu_1) + (1-\tau)X_n \tag{21}$$

where $0 < \tau < 1$. The control system of (5) becomes

$$\begin{cases} x_{n+1} = \tau\left(x_n + \mu_1(r_1 x_n \ln\frac{k_1}{x_n} - \eta_1 x_n y_n)\right) + (1-\tau)x_n, \\ y_{n+1} = \tau(y_n + \mu_1(\beta_1(1-e^{-a_1 x_n})y_n - \delta_1 y_n)) + (1-\tau)y_n, \end{cases} \tag{22}$$

The Jacobian matrix at $\varsigma_2(x^+, y^+)$ is written as follows

$$J(x^+, y^+) = \begin{pmatrix} 1-\breve{\varkappa} & -x^+\eta_1\mu_1\tau \\ a_1 e^{-a_1 x^+} y^+ \beta_1\mu_1\tau & 1+\left(1-e^{-a_1 x^+}\right)\beta_1\mu_1\tau - \delta_1\mu_1\tau \end{pmatrix}$$

where $\breve{\varkappa} = \left(r_1 + y^+\eta_1 + r_1 \ln\left[\frac{k_1}{x^+}\right]\right)\mu_1\tau$.

The eigenvalues of the above Jacobian matrix satisfy the following equation.

$$\lambda^2 + \ddot{\chi}_1\lambda + \ddot{\chi}_0 = 0 \tag{23}$$

where $\ddot{\chi}_1 = -2 + \left(r_1 - \beta_1 + e^{-a_1 x^+}\beta_1 + \delta_1 + y^+\eta_1 - r_1 \ln\left[\frac{k_1}{x^+}\right]\right)\mu_1\tau$

$\ddot{\chi}_0 = Det\left(J(x^+, y^+)\right)$

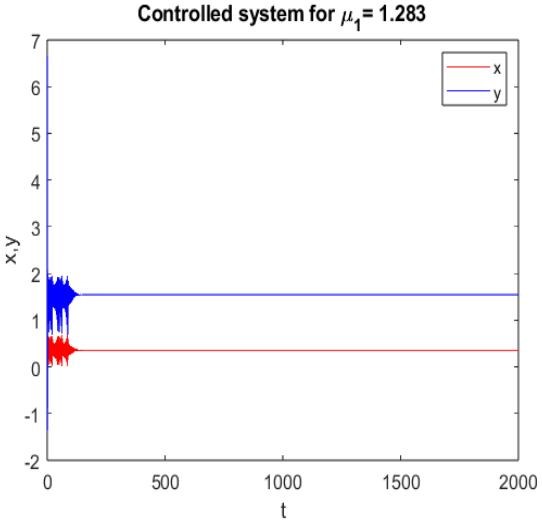

(a)

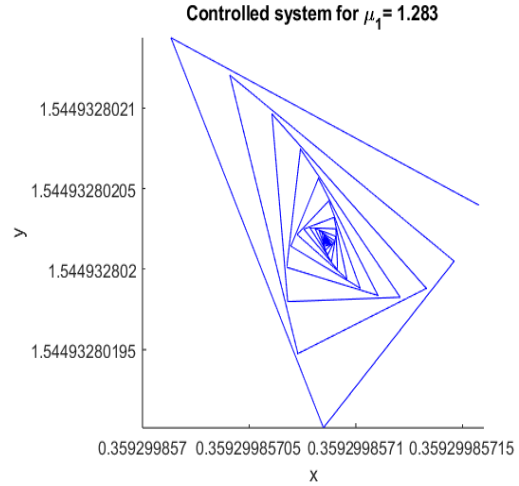

(b)

Fig. 3. Chaos control of the system (22) (a) Time trajectory (b) Phase picture.

Lemma 3. *If the roots of (23) are inside an open disc and the conditions in Lemma 1 are satisfied, then the controlled system (22) is a sink (stable) for the unstable uncontrolled system's fixed point* $\varsigma_2(x^+, y^+)$.

Illustration 2. We choose $r_1 = 1.45, k_1 = 1.16, a_1 = 1.25, \eta_1 = 1.10, \beta_1 = 1.1, \delta_1 = 0.01$ and $\mu_1 = 1.2125 < \mu_{1PD}$ to assess the effectiveness of hybrid control strategy. We observe that the fixed point of the model (5) is unstable. The fixed point turns into a sink for $\tau = 0.999998$ for the controlled system (22) which reduces the chaotic dynamics (see Figure 3).

VII. Conclusions

To create a more accurate portrayal of predator-prey interactions in ecological systems, a mixed functional response can be added to a discrete prey-predator model. It's crucial to remember that the specific traits of the predator and prey species being modeled should guide the selection of functional responses. Furthermore, mixed functional responses add more complexity even as they boost realism. The qualitative study of a predator-prey model with mixed functional responses in discrete time is the subject of this paper. The manuscript presents our findings in full and offers a thorough stability analysis of these equilibrium points.

Using the center manifold theorem and bifurcation theory, we determined the requirements for the occurrence of a PD bifurcation and an NS bifurcation of the map (5) at a positive fixed point. Phase portraits, bifurcation diagrams, and other analytical tools have been utilized to examine additional dynamic characteristics of the system (5). In particular, system (5) displays dynamical behavior when the range of parameters changes. A PD bifurcation within the model demonstrates the evolutionary dynamics of predator and prey populations. The transition from a stable state to chaotic behavior is associated with this bifurcation, highlighting the widespread occurrence of chaos across various natural systems and phenomena. Lastly, the hybrid control approach is used to stabilize the chaotic orbits at an unstable fixed point. To sum up, this paper provides a thorough examination of the dynamics of a model system and shows that, under certain parametric circumstances, bifurcations and chaos can occur. For this discrete system, further investigation is warranted to explore other properties such as synchronization and co-dimension-2 bifurcation.

Funding: This research is made possible by funding from the Centennial research grant of University of Dhaka (DU), Dhaka, Bangladesh.

Conflict of interest: There is no conflict of interest declared by the authors.

References

1. Baurmann M., T. Gross and U. Feudel, 2007. Instabilities in spatially extended predator-prey systems: spatio-temporal patterns in the neighborhood of Turing-Hopf bifurcations, *Journal of Theoretical Biology*, **245(2)**, 220–229.
2. Malthus T. R., 1798. An Essay on the Principle of Population, as it affects the future improvement of society. With Remarks on the Speculations of Mr Godwin, M. Condorcet, and other writers, *Kelley, Bloomington, Indiana, Harmondsworth: Penguin, 7th edition*.
3. Lotka A. J., 1925. Contribution to the theory of periodic reactions, *J. Phys. Chem.* **14**, 271–274.
4. Volterra V., 1926. Fluctuations in the abundance of a species considered mathematically, *Nature* **118**, 558– 560.
5. Rosenzweig M. L., and R. H. MacArthur, 1963. Graphical representation and stability conditions of predator–prey interactions, *Am. Nat.* **97**, 209– 223.
6. Holling C. S., 1965. The functional response of predator to prey density and its role in mimicry and population regulation, *Mem. Entomol. Soc. Can.* **45**, 1–60.
7. He Z. and B. Li, 2014. Complex dynamic behavior of a discrete-time predator–prey system of Holling-III type, *Adv. Diff. Eqs. 2014*, 180–193.
8. Zhang L., C. Zhang, and M. Zhao, 2014. Dynamic complexities in a discrete predator–prey system with lower critical point for the prey, *Math. Comput. Simulat.* **105**, 119–131.
9. Hu D., and H. Cao, 2015. Bifurcation and chaos in a discrete-time predator–prey system of Holling and Leslie type, *Commun. Nonlin. Sci. Numer. Simulat.* **22**, 702–715.
10. Yildiz S., S. Bilazeroglu, and H. Merdan, 2023. Stability and bifurcation analyses of a discrete Lotka–Volterra type predator–prey system with refuge effect, *J. Comput. Appl. Math.*, **422**, 114910.
11. Li X., and X. Shao, 2022. Flip bifurcation and Neimark–Sacker bifurcation in a discrete predator–prey model with Michaelis–Menten functional response, *Electron. Res. Arch.* **(31)** 37–57.
12. Kangalgil F., 2019. Neimark–Sacker bifurcation and stability analysis of a discrete-time prey–predator model with Allee effect in prey, *Adv. Difference Equ.* **2019 (1)** 1–12.
13. Seval I., 2019. A study of stability and bifurcation analysis in discrete-time predator–prey system involving the Allee effect. *International Journal of Biomathematics*, **12(1)**, 1950011.

14. Salman S. M. A., M. Yousef, and A. A. Elsadany, 2016. Stability, bifurcation analysis and chaos control of a discrete predator–prey system with square root functional response, *Chaos Solitons Fractals*, **93**, 20–31.

15. Cheng L. and H. Cao, 2016. Bifurcation analysis of a discrete-time ratio-dependent prey–predator model with the Allee effect, *Commun. Nonlinear Sci. Numer. Simul.* **38**, 288–302.

16. Lynch S., 2007. Dynamical Systems with Applications Using Mathematica. *Birkhauser, Boston.*

17. Romeiras F. J., C. Grebogi, E. Ott, and W. P. Dayawansa, 1992. Controlling chaotic dynamical systems. *Phys. D* **58**, 165–192.

18. Luo X. S., G. Chen, B. H. Wang and J. Q. Fang, 2003. Hybrid control of period-doubling bifurcation and chaos in discrete nonlinear dynamical systems. *Chaos Soliton Fract.* **18**, 775–783.

19. Ott E., C. Grebogi and J. A. Yorke, 1990. Controlling chaos. *Phys. Rev. Lett.* **64(11)**, 1196–1199.

20. Kuznetsov Y. A., 2004. Elements of applied bifurcation theorey, *New York: Springer*.

21. Han X. and C. Lei, 2023. Bifurcation and turing instability analysis for a space-and time-discrete predator-prey system with smith growth function, *Chaos Solitons Fract.*, **166**, 112910.

22. Pati N. C., G. C. Layek, and N. Pal, 2020. Bifurcations and organized structures in a predator-prey model with hunting cooperation, *Chaos, Solitons & Fractals*, **140**, 110184.

23. Roy B., S. K. Roy, and M. H. A. Biswas, 2017. Effects on prey--predator with different functional responses, *International Journal of Biomathematics*, **10(8)**, 1950011.

24. Uddin M. J., S. M. S. Rana, S. Işık, F. Kangalgil, 2023. On the qualitative study of a discrete fractional order prey–predator model with the effects of harvesting on predator population, *Chaos, Solitons & Fractals*, **175**, 113932.